FABRICATION AND CHARACTERIZATION OF THIN FILM ON POLYETHYLENE TEREPHTHALATE SUBSTRATE FOR CIGS SOLAR CELL

by

MOHAMMAD GHAFFAR FARAJ

Thesis submitted in fulfilment of the requirements for the degree of Doctor of Philosophy

April 2012

This Dedicated to

Soul of my grandmother-"may Allah rest his soul in peace"

My father and my mother for their prayers,

My wife and my children for their patient, moral support and accepting the inconveniences during the time of this work

ACKNOWLEDGMENTS

First of all, I would like to thank ALLAH for granting me the health, patience, and determination to complete this doctoral study. I would also like to thank my supervisor Professor Dr. Kamarulazizi Ibrahim, for his guidance, time, moral support and critical questions about my research. I consider myself very lucky and most honored to have been one of his students.

I give heartfelt thanks to the School of Physics, Universiti Sains Malaysia. I would also like to express my appreciation for the staff in the Nano-Optoelectronics Research Laboratory for their cooperation.

I owe the deepest gratitude to the Ministry of Higher Education and Scientific Research in the Iraqi Kurdistan government for its support. I also thank the University of Koya, School of Sciences, Faculty of Health and Sciences, Department of Physics for their cooperation and facilities.

I extend my thanks and appreciation to the employees of the School of Chemical Sciences, Universiti Sains Malaysia for accomplishing some of the measurements for my research, and I especially thank Dr. Abdussalam Salhin Mohamed Ali.

The prayers of my father and mother and the patience of my wife, Hamdia, and my two daughters, Solin and Nadin, were powerful sources for my success.

Lastly, my regards to all of those who supported me throughout this project especially Mr. Ahmed Ismail Nanakli.

MOHAMMAD GHAFFAR FARAJ

Penang Island, Malaysia, October 2011

CONTENTS

LIST OF TABLE

LIST OF FIGURES

.

LIST OF ABBREVATIONS

AFM	Atomic force microscopy
Al	Aluminium
AM1.5	Standard terrestrial solar spectrum ‘Air Mass 1.5’
C	Carbon
Cd	Cadmium
CdS	Cadmium sulfide
CIGS	Copper indium gallium selenide
Cu	Copper
$Cu(acac)_2$	Copper (II) acetylacetonate
DC	Direct current
EDX	Energy dispersive X-ray analysis
EHP	Electron-hole pairs
Ga	Gallium
$Ga(acac)_3$	Gallium(III) acetylacetonate
I-V	Current-voltage
In	Indium
$In(acac)_3$	Indium (III) acetylacetonate
IPA	Isopropyl alcohol
mg	Milligram
mL	Milliliter
mmol	Millimole
Mo	Molybdenum
N_2	Nitrogen
Ni	Nickel
O	Oxygen
Pa	Pascal

PC	Polycarbonate
PEN	Polyethylene naphthalate
PET	Polyethylene terephthalate
PL	Photoluminescence
PI	Polyimide
PV	Photovoltaic
RMS	Root mean square
rpm	Revolutions per minute
S	Sulfur
Se	Selenium
TFSC	Thin-film solar cell
TFPV	Thin film photovoltaic cell
W	Watt
XRD	X-ray diffraction
ZnO	Zinc oxide

LIST OF SYMBOLS

c	Speed of light in a vacuum
D_n	Diffusion coefficient
D_p	Diffusion coefficient for holes
E	Electric field
E_c	Bottom edge of conduction band
E_f	Fermi level
E_g	Energy gap
E_v	Top edge of valence band
FF	Fill factor
$F(\lambda)$	Number of incident photons cm^{-2} s^{-1} per unit bandwidth
G_n	Electron generation rate
h	Plank constant
I	Current
I_0	Reverse saturation current
I_L	Light-generated current
I_m	Maximum current
I_{sc}	Short circuit current
J_0	Reverse saturation current density (amperes/cm^2)
J_d	Photocurrent per unit bandwidth
J_n	Electron current density
J_p	Hole current density
k	Boltzmann’s constant
n_p	Photo-generated minimum carrier density
n_{p0}	Equilibrium minority carrier density in the dark

P_{in}	Incident power
P_m	Maximum power
q	Unit electronic charge
R_H	Hall coefficient
R_s	Sheet resistance
R_{sh}	Shunt resistance
$R(\lambda)$	Fraction of these photons reflected from the surface
T	Absolute temperature
V_m	Maximum voltage
V_{oc}	Open circuit voltage
w	Width of the depletion
x_j	Junction depletion
α	Optical absorption coefficient
λ	Wavelength
μ	Mobility
ρ	Resistivity
τ_n	Carrier lifetime for electrons
Φ_m	Metal work function
χ	Electron affinity
ν_n	Electron velocity
ν_p	Hole velocity

FABRIKASI DAN PENCIRIAN FILEM NIPIS ATAS POLIETILENA TEREFTALAT SUBSTRAT UNTUK SEL SURIA CIGS

ABSTRAK

Kos tenaga elektrik yang dihasilkan daripada sel suria adalah lebih tinggi daripada kos tenaga fosil. Pengurangan kos sel suria adalah diperlukan. Kemungkinan untuk memfabrikasi CIGS filem nipis di atas substrat polietilena tereftalit (PET) untuk mengurangkan kos teknologi sel suria CIGS telah dikaji.

Struktur sel suria CIGS yang terdiri daripada substrat polietilena tereftalit (PET), pemantul sentuhan belakang molibdenum, lapisan penyerap CIGS, lapisan penampan kadmium sulfida (CdS) dan lapisan tetingkap zink oksida (ZnO) telah dinilai.

Lapisan sentuhan belakang Mo, dengan ketebalan 800 nm, telah didepositkan di atas substrat PET dengan menggunakan teknik percikan arus terus (DC) sputtering. Kajian permukaan AFM telah menunjukkan yang permukaan lapisan Mo adalah rata, dengan kekasaran permukaan (RMS) 25.09 nm. Rintangan filem tersebut adalah 1.6×10^{-5} Ω.cm. Filem CIGS dengan ketebalan 1.5 μm dengan kandungan Ga yang dinaikkan daripada 0.3 ke 0.6 telah dideposit dengan menggunakan teknik cetakan skrin. Kekasaran permukaan (RMS) filem CIGS tersebut berada dalam jurang 71.35-33.95 nm untuk kandungan Ga (0.3-0.6), dan jurang jalur tenaga filem-filem tersebut meningkat dengan pertambahan nisbah Ga/(In + Ga). Daripada segi ciri-ciri elektrik, filem-filem CIGS dengan kandungan Ga yang berbeza menunjukkan konduktiviti jenis-p.

Filem nipis CdS dengan ketebalan 100 nm telah didepositkan dengan menggunakan teknik penyejatan terma. Keputusan kajian telah menunjukkan bahawa kekasaran permukaan (RMS) filem tersebut adalah 3.46 nm dan kadar transmisi cahaya adalah melebihi 60% untuk panjang gelombang yang melebihi 500 nm. Jurang jalur tenaga filem nipis CdS adalah 2.41

eV. Filem nipis CdS selepas didepositkan mempunyai kerintangan tinggi; sekitar 923 Ω.cm. Keputusan-keputusan ini menunjukkan filem nipis bahawa CdS mempunyai cirri-ciri yang ideal sebagai lapisan penampan dalam sel suria CIGS. Lapisan tetingkap ZnO dengan ketebalan 300 nm telah dikaji dengan menggunakan teknik penyejatan terma. Keputusan kajian menunjukkan kekasaran permukaan (RMS) filem nipis ZnO adalah 16.23 nm dan jurang jalur tenaga filem nipis ZnO adalah 3.375 eV. Filem nipis ZnO selepas didepositkan mempunyai kerintangan 12×10^{-4} Ω.cm.

Arus litar pintas (I_{SC}) bagi sel suria ini menurun dengan peningkatan nisbah Ga/(In+Ga), sedangkan voltan litar terbuka (V_{OC}) meningkat dengan peningkatan nisbah yang sama. Sel suria mempamerkan kecekapan tertinggi 4.122% pada nisbah Ga/(In+Ga) 0.3, bersamaan dengan jurang jalur tenaga (E_g) 1.25 eV, V_{oc} 0.362 V dan I_{sc} 5.64 mA. Ini bakal merintis jalan yang baru bagi memfabrikasi sel suria pada kos yang rendah dan anjal.

FABRICATION AND CHARACTERIZATION OF THIN FILM ON POLYETHYLENE TEREPHTHALATE SUBSTRATE FOR CIGS SOLAR CELL

ABSTRACT

The cost of the electrical energy generated by the solar cells was higher than that generated by fossil fuels. Cost reduction of the solar cell is therefore required. Feasibility of fabricating thin film CIGS solar cells on low-cost polyethylene terephthalate (PET) substrates in order to bring down the costs of the CIGS solar cell technology was explored.

The structure CIGS solar cells consisted of polyethylene terephthalate (PET) substrate, molybdenum back contact reflector, CIGS absorber layer, cadmium sulfide (CdS) buffer layer and zinc oxide (ZnO) window layer have been evaluated.

The Mo back contact layer, with a thickness of 800 nm, was deposited on a PET substrate using direct current (DC) sputtering. The AFM surface study showed that the surface of the Mo films was also smooth, presenting an RMS of 25.09 nm. The resistivity of the films deposited was 1.6×10^{-5} Ω.cm. A 1.5 µm thick p-type CIGS with a Ga content that varied from 0.3-0.6 were deposited using a screen-printing technique. The RMS surface roughness of the CIGS film varied from 71.35-33.95 nm for Ga contents (0.3-0.6), and the band-gap energies of the CIGS thin films increased with an increasing Ga/(In + Ga) ratio. From the electrical properties, it was found that CIGS films with different Ga ratios always show p-type conductivity.

A CdS thin film with a thickness of 100 nm was deposited using a thermal evaporation technique. It was found that the RMS for the CdS thin film was 3.46 nm,

and the transmission rate was more than 60% for wavelengths longer than 500 nm. The band gap for the CdS thin film was 2.41eV. The as-deposited CdS thin film had a high resistivity of 923Ω.cm.These results show that the CdS thin film has properties that make them ideal as a buffer layer in CIGS solar cells. The ZnO window layer with a thickness of 300 nm was studied using a thermal evaporation technique. It was found that the RMS for the ZnO thin film was 16.23 nm, and the band gap for the ZnO thin film was 3.375 eV. The as-deposited ZnO thin film had a resistivity of 12×10^{-4} Ω.cm. These results show the ZnO thin film has properties that make them ideal as a window layer in CIGS solar cells.

The short-circuit current (I_{SC}) of the solar cell decreased with the Ga/(In+Ga) ratio, while the open-circuit voltage (V_{OC}) increased with this ratio. The solar cell exhibited its highest efficiency of 4.122% at a Ga/(In+Ga) ratio of 0.3, corresponding to an E_g of 1.25 eV, a V_{OC} of 0.362 V and an I_{SC} of 5.64 mA. This may open a new way for fabrication of low cost and flexible solar cell.

CHAPTER 1

INTRODUCTION

1.1 Overview

Solar cells are now the most important and viable power source for space vehicles, such as satellites and shuttles. This source of power has also been used in large-scale terrestrial power generation applications to successful effect. As the energy consumption in the world grows each year, most of the energy comes from petroleum, natural gas, fossil fuels and nuclear power generation. These power systems are polluting, costly, or will be exhausted in the near future. Therefore, a renewable energy source, such as solar energy, is needed to replace these systems and protect our natural environment and future use. Photovoltaic (solar) energy conversion is an excellent candidate because it is clean, inexhaustible, uninterruptible, and non-polluting.

Solar cells use the internal photovoltaic (PV) effect in semiconductors and are capable of providing electricity directly from the sun for many different uses, with the added benefit of power generation for longer periods of time at a lower maintenance cost.

Recent interest has increased the amount of effort put into the development of and research on affordable flat-panel solar cells, along with concentrator systems and thin film PV devices. Many other innovative concepts are also under consideration. As a simple definition, the basic function of a solar cell module is to absorb incident sunlight and to create electron-hole pairs that collect at the outer contacts of the solar cells to produce electricity for many different uses. A semiconductor p-n junction structure is commonly used in solar cells. The useful spectral range for converting the incident sunlight into electricity can be calculated using the band gap (E_g) of the semiconductor. Separation and transport of the photo-generated electron-hole pairs are accomplished by the electric field that automatically forms as a part of the p-n junction. A transparent conductive oxide (TCO) or ohmic contact grid is normally used for current collection in the front, and a metal contact is used on the backside of the solar cell.

After Chapin, Fuller and Pearson described the first silicon solar cell in 1954, the solar cell has evolved from being a low-efficiency device to being a major power generation source for spacecraft and many terrestrial power generation systems. Currently, high efficiency solar cells (both single-junction and multi-junction) are based on semiconductors of III-V compounds, such as the GaAs- and InP- materials that have been developed for space applications, while crystalline silicon solar cells are still the dominant PV technology for terrestrial power generation applications. The commercial silicon solar cells available today are made from solar-grade single crystalline silicon or polycrystalline silicon materials. Although high efficiencies are achieved with single crystalline silicon, the silicon technology is not expected to become a low-cost PV technology. One reason is that silicon is an indirect band gap semiconductor that requires a thick absorber layer (about 250-400 μm thick) to absorb 90% of the useful sunlight for electricity generation.

In the past few years, much effort has been devoted to developing various low-cost, high-efficiency and reliable solar cells for usage in multiple fields, such as terrestrial and space power generation as well as for use in consumer electronics. Efficient solar cells can be made by thin film technology. By using semiconductor materials with high absorption, a film thickness of a few micrometers is adequate and collects sunshine effectively. A wide variety of absorber materials are available for solar cell applications.

The a-Si:H films are easy to dope, as all that must be added are gases that contain phosphorus or boron during the process of deposition for p-type and n-type doping. The optical band gap of a-Si can be tuned and is usually approximately $Eg \approx 1.7eV$. The a-Si:H thin film solar cells are efficient to a percentage of 13.1%, though long-term stability is a key issue for this type of solar cell.

Other thin film PV technologies that have their basis in cadmium telluride (CdTe) (which has a maximum efficiency of 16.5% (Romeo et al., 2004)) and CdS/ $CuIn(Ga)Se_2$ (CIGS) material systems have shown great promise for large-scale terrestrial power systems.

CIGS thin film solar cells with efficiencies exceeding 19% at standard terrestrial solar spectrum (Air Mass 1.5) have been demonstrated recently by the National Renewable Energy Laboratory research team (Ramanathan et al., 2005). Thin-film PV technology benefits from a low material consumption and price compared to crystalline silicon solar cells. Scaling the PV technology from single solar cells to large-area PV modules is straightforward because many cells can be interconnected from material deposited on one substrate in the form of stacked film layers. Compared to the crystalline material, thin film solar cells can be manufactured with less energy input. This shortens the energy payback time (the time needed for the photo-generated energy output to equal the energy consumed to produce the device).

Specific advantages of the $CuInGaSe_2$ alloy are its wide compositional tolerance and the fact that it contains a direct band gap material with high visible spectrum optical absorption. Two key factors that make a difference to the compatibility of a solar cell are its cost and conversion efficiency.

The thin film solar cells provide the best hope for obtaining PV devices with high efficiency and low cost. Two films, copper indium diselenide and copper indium gallium diselenide (known as CIS or CIGS, respectively) are the most promising materials of all thin film solar cells for achieving these goals. Such materials have certain exceptional characteristics that are particularly suitable for photovoltaic heterojunction applications.

1.2 Problem statement

Photovoltaic is a very promising field amount various renewable energies. But solar cells can only establish themself durable on the market, if they are also economically profitable. R& D not only focusing on enhancing the conversion efficiency and the stability of the solar cells, but is also trying to find processes and technologies to reduce the costs.

Presently, the cost of the substrate (e.g., glass, steel, and polymers) for thin film solar cells is one of the factors substantially influencing the production cost of modules. Flexible substrates offer a number of possibilities for the usage of solar cells. For instance, they can be applied for structural integration when used on uneven surfaces, such as tiles or bricks. Additionally, these kind of cells are both lightweight and thin (Bloss et al., 1995). Because of their flexibility, they are more useful than rigid cells. Flexible cells are also the primary choice for space applications because they can be used to construct simpler mechanisms for deployment. This saves weight and reduces the cost of launches by a significant amount. Another advantage of flexible solar cells, and maybe the most important one, is the potential to reduce production costs. A low-cost and light weight substrate, in combination with a suitable flexible encapsulant, would combine the advantages of flexible solar cells, cost-effective production and low energy pay-back time.

1.3 Objectives of the research

The objectives of this research are as follows:

1. To prepare chalcopyrite copper indium gallium diselenide (CIGS) ink with dissolved copper, indium, gallium acetylacetonate and Se powder in oleylamine using hot injection methods.
2. To study the structural, optical and electrical properties of molybdenum deposited on a PET substrate.
3. To study the structural, optical and electrical properties of CIGS as an absorber layer at room temperature and deposited using the screen-printing technique.
4. To study the effects of the Ga content in a CIGS absorber layer on the structural, electrical and optical properties of the corresponding thin films.
5. To study the structural, optical and electrical properties of CdS as a buffer layer using the thermal evaporation technique.
6. To study the structural, optical and electrical properties of ZnO as a window layer using the thermal evaporation technique.
7. To fabricate CIGS solar cells on a PET substrate.
8. To study the effects of the Ga content in a CIGS absorber layer on the photovoltaic properties of CIGS solar cells.

1.4 Research originality

The novel contributions of this research are listed below.

1. Use of polyethylene terephthalate (PET) as a substrate for CIGS solar cells.

PET plastic has been selected as a substrate in this work for the following reasons: PET is one of the least expensive plastic substrates available (less expensive than polyimide), PET is compatible with the deposition conditions for thin film solar cells (temperature and degassing) and the use of PET plastic as a substrate for thin-film solar cells (silicon, indium tin oxide, zinc oxide) is documented in the literature (Bailat et al., 2005; Haug et al., 2009; Rath et al., 2010; Wong et al., 2004; Lu et al., 2007). However, the fabrication of CIGS thin film solar cell on a PET substrate has not been reported in the literature.

2. Preparation of CIGS thin films using the screen-printing technique at room temperature. The polymer materials that are used as flexible substrates require low temperature (< 250 ^{0}C) processes, where the quality of the inorganic films is generally poor when compared with high temperature (> 400 ^{0}C) processes. There has been a great deal of research dedicated to finding a way to obtain high-quality films at low temperatures by developing new deposition technologies and improving the deposition processes, including sputter deposition (Henry et al., 2001), electron beam deposition (Deng et al., 2000), and PECVD (Rochat et al., 2003). In this work, after preparing the CIGS ink using hot injection methods, a CIGS thin film will be prepared at room temperature using screen printing. The screen-printing technique is a method with many benefits because large-area films with a great deal of uniformity can be produced without much expenditure. The use of CIGS thin films prepared at room temperature using screen printing has not been reported in the literature.

3. Preparation of CdS buffer layer using the thermal evaporation technique.

In most laboratories, the standard device structure of Cu(In,Ga)Se_2 (CIGS)-based solar cells includes a thin chemical bath–deposited (CBD) CdS buffer layer between the CIGS absorber layer and the transparent ZnO front electrode (Hashimoto et al., 1998). Many studies have used films based upon ZnS, In_2S_3, and In_2Se_3 that were deposited using thermal evaporation on absorbers and tested as an alternative to the traditional CdS buffer (Strohm et al., 2005; Barreau et al., 2003; Gall et al., 2005; Luo et al., 2009).Thermal evaporation is one suitable method for depositing CdS large-area thin films for solar cell applications (Chavez et al., 1997; Derin et al., 2009). Preparation of CdS buffer layer using the thermal evaporation technique has not been reported in the literature.

4. Preparation of ZnO window layer using the thermal evaporation technique.

Most studies have used ZnO thin films in CIGS solar cells using the method of RF sputtering. A number of studies have used other methods to prepare ZnO thin films as the window layer, such as the MOCVD (Sang et al., 2003) and ALE methods (Stolt et al., 1994). Preparation of ZnO window layer using the thermal evaporation technique has not been reported in the literature.

1.5 Literature review on CIGS thin film solar cells

The compounds $CuInSe_2$ (CIS) and Cu(In, Ga)Se_2 (CIGS), with their chalcopyrite structure, have the greatest potential when utilized in thin film solar cells (Wang et al., 2010; Saji et al., 2011). The main advantages of CIS/CIGS-based solar cells are the low cost of the materials used and the conversion efficiency.

Copper indium diselenide ($CuInSe_2$) is a member of the I-III-VI_2 family, a semiconductor family with a chalcopyrite structure and a direct energy band gap of approximately 1.02 eV at room temperature (Sobotta et al., 1980; Hörig et al., 1978). Its excellent thermal stability, radiation hardness and high optical absorption coefficient make it an ideal candidate material for efficient and low cost thin film solar cells for both single and tandem junctions (Rockett and Birkmire, 1991).

Solar cells based upon vacuum-evaporated CIS films have been fabricated with a conversion efficiency of more than 14.5% (AbuShama et al., 2004). The primary limits to CIS-based device efficiency are reproducibility, large area uniformity and the slightly less than optimum band gap. However, research is in progress to improve the efficiencies of the devices by improving their uniformity and developing better deposition techniques.

Copper gallium diselenide ($CuGaSe_2$, CGS) is another member of the I-III-VI_2 semiconductor family and has properties that are very similar to CIS in terms of its structural and electrical behavior. It has a direct band gap of 1.68 eV (Hörig et al., 1978; Orsal et al., 2000; Young et al.,2003).

Thin film polycrystalline solar cells based upon the ternary chalcopyrite compounds CIS and CGS have been shown to have acceptable photovoltaic properties. However, the fundamental limit on the efficiency of $CuInSe_2$-based solar cells is the small open circuit voltage, which is due to the 1.02 eV band gap values of the absorber layer; the optimum value is 1.5 eV.

The CIS band gap can be fine-tuned toward the desired value by partially substituting gallium in place of indium. The band gap of the resultant $CuIn_{1-x}Ga_xSe_2$ (CIGS) can be increased continuously from 1.02 eV (for pure CIS) to 1.68 eV (for pure CGS) by varying (x) between zero and one (Zegadi et al., 1992). CIGS has a high coefficient of light absorption ($>10^4$ cm^{-1}) in the visible region of the electromagnetic spectra. CIGS is a direct band gap material. The standard thickness of the CIGS layer in a solar cell is presently 1.5–2 μm (Hou et al., 2009). Various techniques of depositing CIGS thin films have been reported, including vacuum evaporation (Chenene and Alberts, 2003), spray pyrolysis deposition (Shirakata et al., 1999), electrodeposition (Bhattacharya et al., 2000), close-spaced vapor transport deposition (Bouloufa et al., 2009), sputtering deposition (Shi et al., 2011), electron beam deposition (Venkatachalam et al., 2009) and the screen-printing technique at high temperature (575 ^{0}C) (Wada et al., 2006).

The process of the development of CIGS films on flexible substrates is considered to be intriguing because of the portable, small volume, damage-free and lightweight nature of these devices. Therefore, CIGS solar cells on flexible polymer substrates are lightweight and can be used effectively for space applications (Kessler et al., 2005;Otte et al., 2006).

CIGS ink is synthesized using commercial-grade copper, indium, gallium acetylacetonate, selenium powder and oleylamine. The basic principles of the preparation of CIGS ink in this work are given in the literature (Hergert et al., 2006; Park et al., 2006; Matsushita and Takizawa, 1997; Tang et al., 2008; Panthani et al., 2008).

Some researchers have used CIGS ink chemically for the fabrication of CIGS solar cells. V.K. Kapur et al. (Kapur et al., 2004) prepared CIGS solar cells through the use of precursor inks based in water; these are colloidal suspensions of tiny particles of mixed oxides of Cu, In and Ga. It has been observed that the best efficiencies produced with this process are on polyimide (8.9%), Mo foil (13.0%) and glass (13.7 %).

T. Wada et al. (Wada et al., 2006) were responsible for the preparation of a fine $Cu(In,Ga)Se_2$ (CIGS) powder, which was used for screen printing through a mechanochemical process. A screen printing technique is used to deposit particulate precursors in a thin layer. The precursor layer was sintered at about 575 °C under a N_2 gas atmosphere; preliminary CIGS solar cells were fabricated on soda-lime glass substrates. The result showed an efficiency of 2.7%, a V_{oc} of 0.325 V, and a J_{sc} of 28.3 mA/cm^2.

Matthew G. Panthani et al. (Panthani et al., 2008) synthesized $CuInS_2$, $CuInSe_2$, and $Cu(In_xGa_{1-x})Se_2$ (CIGS) nanocrystal "inks" for printable photovoltaics. Using films of $CuInSe_2$ nanocrystals as the absorber layer in conventional layered Mo/$CuInSe_2$/ CdS/ZnO/ITO PV devices gave reproducible photovoltaic responses with power conversion efficiencies of up to 0.2%.

Qijie Guo et al. (Guo et al., 2008) developed $CuInSe_2$ nanocrystal and nanoring inks for low-cost solar cells on a glass substrate. The highest efficiency recorded with cells that were fabricated with this patented process was 3.2%.

Table 1.1 Summary of the used of CIGS ink chemically for the fabrication of CIGS solar cells.

References	Materials	Substrate	Efficiency (%)	Temperature (^{0}C)
V.K. Kapur et al.	CIGS	Polyimide, Mo, glass	8.9, 13, 13.7	420-450
T. Wada et al.	CIGS	glass	2.7	575
Matthew G. Panthani et al.	$CuInS_2$, $CuInSe_2$,and $Cu(In_xGa_{1-x})Se_2$	glass	0.2	240
Qijie Guo et al.	$CuInSe_2$	glass	3.2	450-550

1.6 Outline of the thesis

The thesis is structured as follows:

Chapter 1 deals with a brief introduction to solar cells and literature review of CIGS thin film solar cells.

Chapter 2 presents thin film solar cells and the theory of solar cells.

Chapter 3 covers the experimental methodologies, the fabrication techniques and equipment for measurements, which were used in processing and characterizing.

Chapter 4 presents the results of materials in structure CIGS thin film solar cell.

Chapter 5 presents the results of fabrication of CIGS solar cells on PET substrates.

Chapter 6 lists the conclusions and recommendations for future work.

CHAPTER 2

PHYSICS OF SEMICONDUCTOR AND SOLAR CELL

2.1 Introduction

Thin film solar cells (TFSCs) can be used on land for the supply of electricity, and they provide a wide range of options in the design and assembly of a device. A large number of materials are in use for layering of different films using various methods (Chopra et al., 2004).

Thin film solar cells require layers that are between 1.5 and 4 μm thick for light absorption, as opposed to crystalline silicon, which has a thickness in the range of ~180-300 microns. The thickness can be reduced to such an extent mainly because the light-absorbing semiconductor has a direct band gap, as opposed to silicon, which is an indirect band gap semiconductor. The main features for the cost reduction are as follows:

1. The lower thickness requirement of the active light absorption semiconductor layers reduces material costs. Additionally, the purity of the materials is not required to be as high as those for crystalline silicon. A higher purity is essential in silicon as electron-hole pairs are generated away from the built-in electric field and must travel comparatively long distances; if impurities are present, they reduce the diffusion length of these charge carriers. In contrast, thin film solar cells have most of their electron-hole pairs generated in the vicinity of a built-in electric field, and they separated by drift rather than diffusion. Hence, relatively low-purity materials can be used.
2. The use of thinner layers reduces the materials costs.

2.2 Semiconductors

A material whose conductivity is between that of a highly conductive metal and a highly resistive insulator is called a semiconductor. Semiconductors can be classified as either intrinsic or extrinsic, depending upon their purity. They can also be classified as single crystalline, polycrystalline or amorphous based upon their structure. In addition, semiconductors are called n-type or p-type, based upon whether the majority of the carriers are electrons or holes.

The electrical conductivity of a semiconductor can be changed by doping it. Doping is the process of adding impurities to a semiconductor to increase the concentration of charge carriers, thereby improving its conductivity. A semiconductor is said to be extrinsic if it has excess electrons or holes due to either ionized donor impurities or ionized acceptor impurities, respectively. An insulator semiconductor is one in which free electrons in the conduction band or free holes in the valence band are created purely by thermal excitation across the band gap. When a semiconductor is highly doped, such that the Fermi level lies within the conduction or the valence bands, the semiconductor is said to be degenerate.

The band gap E_g of a semiconductor is the difference between the energies of the highest valence band and the lowest conduction level. It is known as the forbidden gap as there are no permissible energy states within the band gap. The band gap of a semiconductor determines the interaction of light with the semiconductor. In general, the band gap of most semiconductors decreases with increasing temperature, given by the following equation (Sze, 1981):

$$E_g = E_g(0) - \frac{\alpha T^2}{T + \beta} \qquad (2.1)$$

Where E_g (0) is the band gap at (0) Kelvin, and T is the absolute temperature while α and β are the fitting parameters.

2.3 p-n junction

In a traditional solar cell, there are three processes involved in the generation of current: the absorption of photons and the generation of electron-hole pairs (EHP) and the collection of carriers. After the carrier generation, the electrons and holes separate and are collected at the contacts. The charge carrier separation has two criteria: the drift of carriers, caused by the integral electrostatic area of a p–n junction, and the dissemination of carriers from high to low zones of carrier concentration following an electrochemical potential gradient. Figure 2.1 illustrates a p-n junction in a schematic diagram.

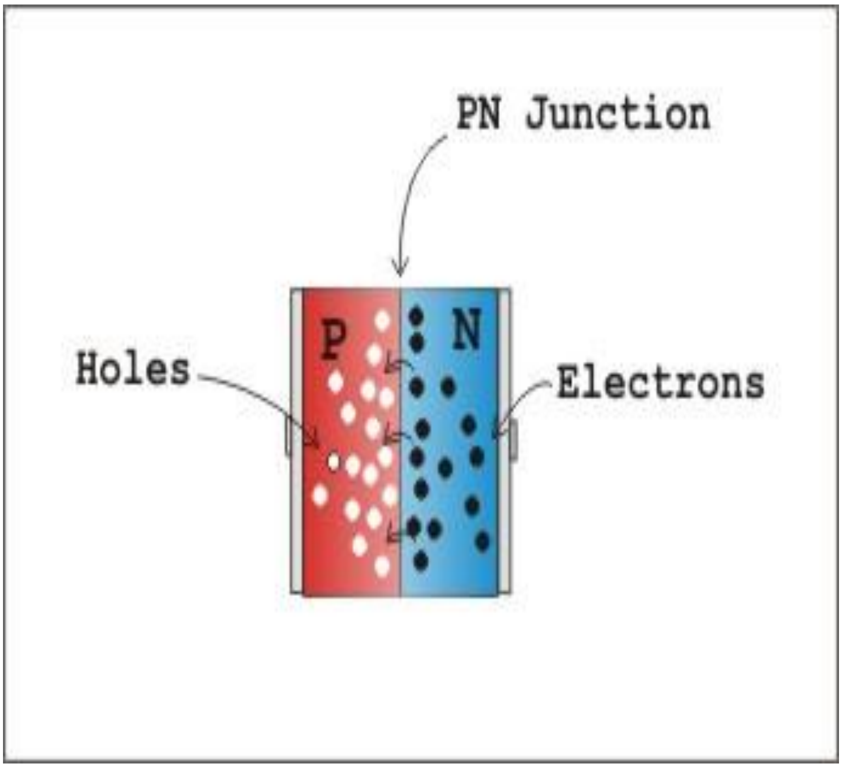

Figure 2.1 Schematic diagram of a p-n junction.

2.4 Heterojunctions

A heterojunction is a junction created between two diverse semiconductor materials. Based upon whether the type of conductivity for both materials is the same or different, heterojunctions can be classified as isotype or anisotype, respectively. Heterojunctions have been extensively studied and used in applications such as photo detectors, light emitting diodes, and solar cells (Sze, 1981). The two materials forming the heterojunction have different band gaps E_{g1} and E_{g2}, different permittivities ε_1 and ε_2, different work functions Φ_{m1} and Φ_{m2} and different electron affinities χ_1 and χ_2, as shown in Figure 2.2. Work function and electron affinity are defined as that energy required to remove an electron from the Fermi level E_f and from the bottom of the conduction band E_c, respectively, to a position just outside the material (vacuum level).

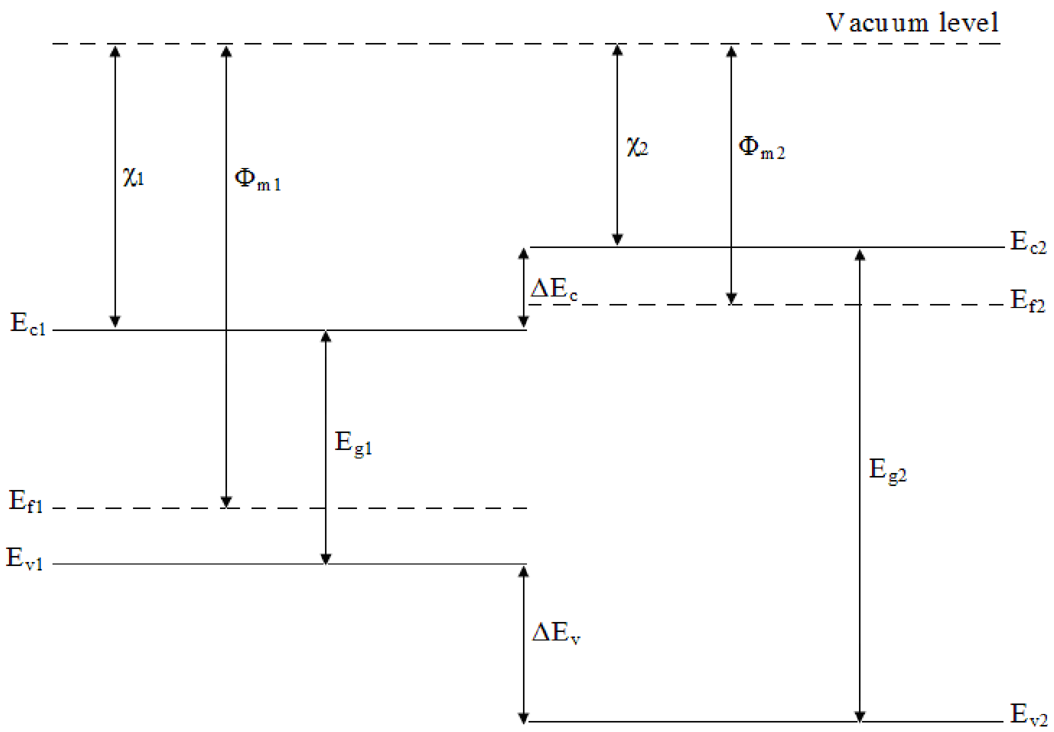

Figure 2.2 Energy band diagram for two isolated semiconductors [adapted from Sze, (1981)].

When a junction is formed between these two materials, the energy band gap diagram appears, as shown in Figure 2.3.

We can observe a higher anomaly located on the conduction spectrum called the conduction band offset. This offset acts as a barrier to the electron flow that begins on the p-side and heads toward the n-side of the junction when illuminated. The magnitude of the conduction band offset is given by the following equation:

$$\Delta E_C = \chi_1 - \chi_2 \tag{2.2}$$

where ΔE_C is the difference in energy of the conduction-band edges in the two semiconductors.

To obtain the optimum current flow in a solar cell, the ΔE_C must be minimized by choosing an appropriate junction partner for the absorption layer. Similarly, the valence band discontinuity is given by

$$\Delta \mathrm{E_v} = \left(\mathrm{E_{g1}} - \mathrm{E_{g2}} - \Delta \mathrm{E_c}\right) \tag{2.3}$$

where ΔE_v is the difference in energy of the valence-band edges in the two semiconductors.The total built in potential, V_{bi}, is equal to the sum of partial built in voltages (V_{b1} and V_{b2}), where V_{b1} and V_{b2} are electrostatic potentials of two semiconductors.

Heterojunctions also suffer from lattice mismatches and differences in electron affinities, which cause interface states at the junction that act as recombination centers. To obtain the maximum performance from the device, these offsets and mismatches must be minimized. The factors that govern the mismatches are primarily the inherent properties of the semiconductor material.

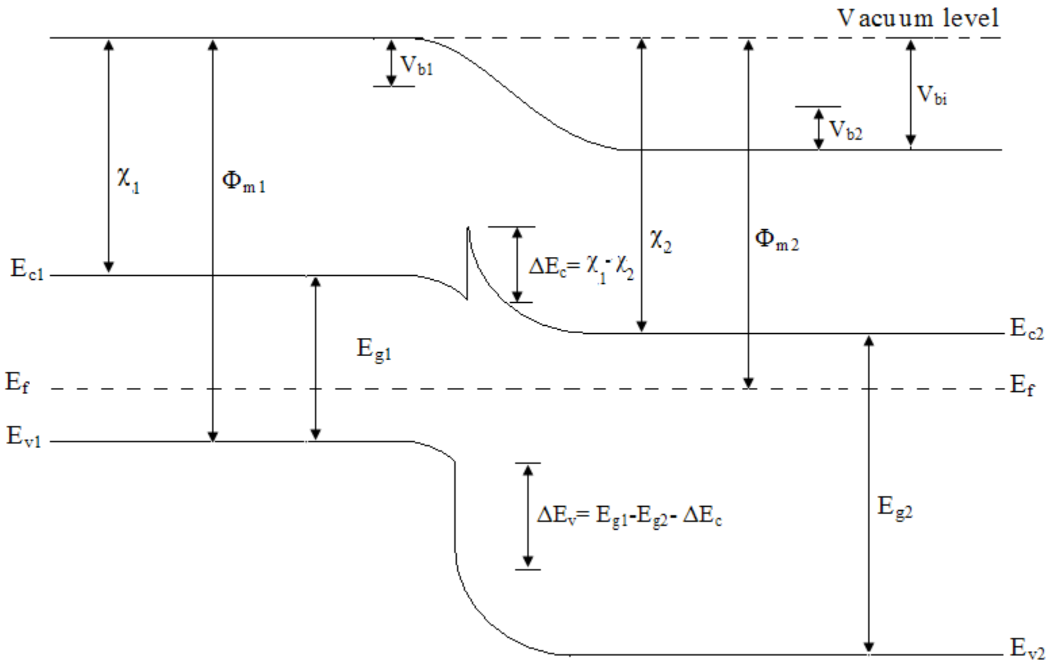

Figure 2.3 Energy band diagram of an ideal p-n anisotype heterojunction at thermal equilibrium [adapted from Sze, (1981)].

The CIGS/CdS solar cell, which is the subject of study here, is an anisotype heterojunction.

The schematic energy band diagram of a particular CIGS/CdS/ZnO heterojunction solar cell structure is displayed in Figure 2.4.

ZnO is the window layer. Because of its high band gap, almost all the light passes through to the underlying layers. Most of the incident light passes through the wider band gap CdS and is diffused in the lower band gap CIGS absorber layer, where it is absorbed. This structure has the advantage of reducing recombination at the front contact as most of the carriers are generated in the absorber.

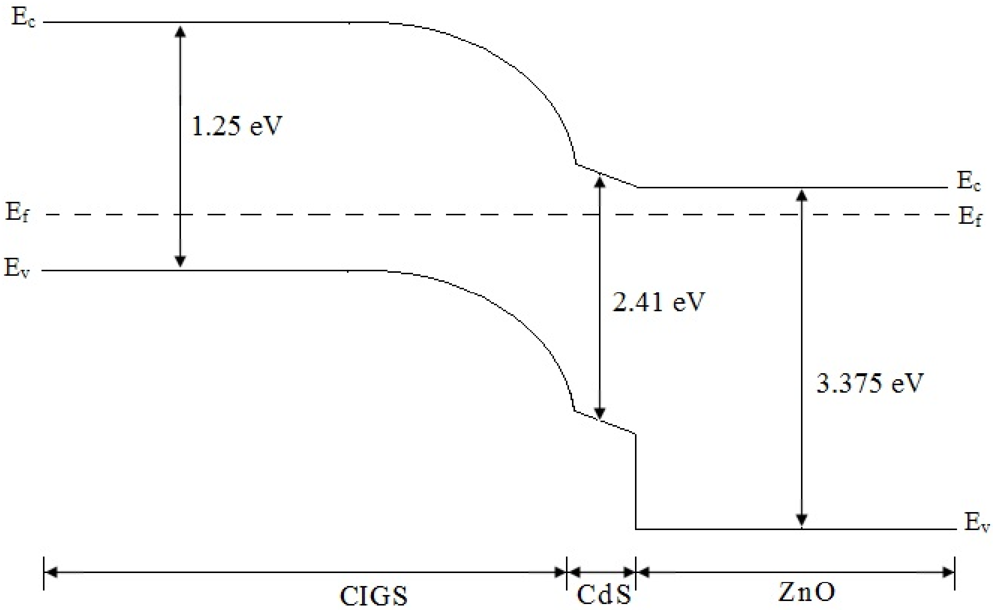

Figure 2.4 The schematic energy band diagram of a CIGS /CdS/ZnO heterojunction solar cell [adapted from Panse, (2003)].

2.5 Solar cells

2.5.1 Theory of operation

Solar cells utilize the photovoltaic effect, wherein sunlight is converted into electrical energy. Solar cells operate in such a manner that they absorb the photons and create electron-hole pairs for semiconductors. These carriers then diffuse to the brink of the depletion site. The electric field acting across the depletion area separates the carriers and helps in the collection of the carriers at the contact.

A solar cell consists of a thin, heavily doped emitter or window layer on top of a relatively thick, moderately doped base or absorber layer. The doping of these two layers proceeds in opposite directions. To maximize the efficiency of the thin film solar cell, certain conditions or requirements must be met (Möller, 1993). The first requirement is that a major portion of the incident light must be taken in by the cell to produce electron-hole pairs. The second requirement is that the solar cell structure must provide a mechanism of separating the generated charge carriers. It is also imperative that the minority carrier lifetimes are sufficiently high so as to ensure good collection efficiency. This is the third requirement.

Excess electron-hole pairs can be generated either by having an absorber layer that is thicker than the absorption length or by light trapping. The assimilation of light by the semiconductor depends upon the energy of the incident photon. A semiconductor only absorbs the light when the energy of the incident photon is larger than the band gap of the semiconductor. This can be summarized as follows:

$$E = \frac{hc}{\lambda} > E_g \qquad (2.4)$$

where h is Plank's constant, c is the speed of light in a vacuum, λ is the wavelength of the incident radiation and E_g is the band gap of the material. The absorption of light by a semiconductor is governed by the following equation:

$$I = I_0 e^{-\alpha t} \qquad (2.5)$$

where I_0 is the intensity of the light incident on the semiconductor, t is the depth of the material from the surface of incidence and α is the absorption coefficient.

The excess electron-hole pairs produced as a result of the absorption of light are swept by the electric field in the depletion area. This provides the required mechanism to separate the photo-generated carriers. However, most of the solar cell employs a shallow junction, and thus most of the light is absorbed by the absorber. Hence, most of the separated charge consists of electrons from the absorber. A few electron-hole pairs are produced in window layer, in the blue region of the incident light. However, the pairs do not make a large contribution to the photocurrent as a result of the heavy doping in the window layer, which greatly reduces the diffusion length of the holes.

To achieve high carrier lifetimes, the absorber must have low defect densities and moderate doping. Higher doping results in the reduction of the carrier lifetime through recombination in bulk; the electric field in the depletion region is directly proportional to the doping concentration. Therefore, an optimum value of doping must be chosen to achieve sufficiently high electric fields with sufficient carrier lifetimes. This process is depicted in Figure 2.5, which shows the energy band structure of a solar cell under illumination.

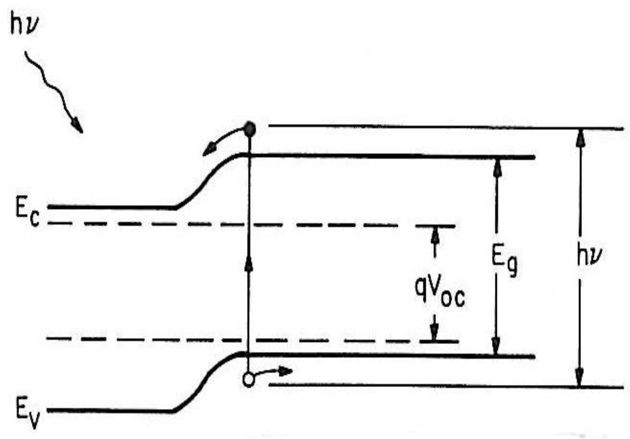

Figure 2.5 Energy band diagram of a p-n junction solar cell under illumination [adapted from Sze, (1981)].

A cell with band gap E_g when exposed to the solar spectrum, a photon with energy greater than E_g , the photon is absorbed. The absorbed photon gives rise to Electron-Hole pairs (EHP). These excess carriers are swept across the junction by the electric field and are collected at the contacts. (Sze, 1981). E_c and E_v are the conduction and valence band edges. The photo-generated excess charge produces a voltage across the external circuit. This voltage is defined as the open-circuit voltage of the solar cell.

2.5.2 Photocurrent and spectral response

The production of electron-hole pairs at a distance x from the surface of the semiconductor, due to the photon absorption of wavelength λ is as follows (Sze, 1981) :

$$G(\lambda) = \alpha(\lambda)F(\lambda)[1 - R(\lambda)]e^{-\alpha(\lambda)x} \tag{2.6}$$

where F (λ) = the number of incident photons cm^{-2} s^{-1} per unit bandwidth, α (λ) is the absorption coefficient, and R (λ) is the fraction of these photons reflected from the surface. In low infusion circumstances, the steady-state continuity equation is as follows (Sze, 1981).

$$\left(\frac{1}{q}\right)\left(\frac{dJ_n}{dx}\right) + G_n - \frac{\left(n_p - n_{p0}\right)}{\tau_n} = 0 \tag{2.7}$$

where J_n is the electron current density, G_n is the electron generation rate, n_p is the photo-generated minimum carrier density, n_{p0} is the equilibrium minority carrier density in the dark and τ_n is the carrier lifetime for electrons.

For electronics in p-type materials, the electron current density J_n is given by

$$J_n = q\, \nu_n\, n_p E + qD_n\left(\frac{dn_p}{dx}\right) \tag{2.8}$$

where E is the electric field, D_n is the diffusion coefficient and ν_n electron velocity. The hole current density is

$$J_p = qv_p\, p_n\, E - qD_p\left(\frac{dp_n}{dx}\right) \tag{2.9}$$

where v_p is the hole velocity and D_p is the diffusion coefficient for holes.

The photocurrent generated in the depletion region is normally unaffected by recombination because the electronic field in the depletion region is greater, and carriers leave it quickly before recombination. The photocurrent per unit bandwidth, or amount of photons taken, is

$$J_{dr} = qF(\lambda)[1 - R(\lambda)]e^{-\alpha(\lambda)x_j}\left[1 - e^{(-\alpha(\lambda)w)}\right] \tag{2.10}$$

where x_j is the junction depletion and w is the width of the depletion layer. The photon-current of a wavelength is the total of the two minority carrier currents and the depletion region current (Sze, 1981).

$$J(\lambda) = J_p\,(\lambda) + J_n(\lambda) + J_{dr}(\lambda) \tag{2.11}$$

The spectral response is equal to this sum total/quantum efficiency for external responses or to qF (1-R) for internally observed responses (Sze, 1981),

$$SR(\lambda) = \frac{1}{qF(\lambda)[1 - R(\lambda)]}\left(J_p\,(\lambda) + J_n(\lambda) + J_{dr}(\lambda)\right) \tag{2.12}$$

once the value of the spectral response is known, the photocurrent density is obtained from the solar spectral distribution F (λ) (Sze, 1981).

$$J_L = q\int_0^{\lambda_m} F(\lambda)\,[1 - R(\lambda)]SR(\lambda)d\lambda \tag{2.13}$$

where λ_m = the highest wavelength, corresponding to the absorber band gap.

2.5.3 Current-Voltage characteristics

Figure 3.6 shows the I-V features of a solar cell in dark and in light. Because the solar cell is a p-n junction diode, its behavior in the dark is governed by the diode equation.

$$I = I_0 \left(e^{\frac{qv}{AkT}} - 1\right) \tag{2.14}$$

where I is the total current, I_0 is the reverse saturation current, k is Boltzmann's constant, A is the diode quality factor, and T is the absolute temperature.

The total current under illumination is given by

$$I = I_0 \left(e^{\frac{qv}{AkT}} - 1\right) - I_L \tag{2.15}$$

where I_L is the light-generated current. The short circuit current I_{sc} is defined as the current flowing in the circuit when the load is shorted. The voltage developed by a solar cell with an infinite load attached to it is called the open circuit voltage (V_{oc}). It is obtained by setting the total current I to 0 in the above equation. The open circuit voltage can be represented by

$$V_{oc} = \frac{AkT}{q}\left(\ln\left(1 + \frac{I_{sc}}{I_0}\right)\right) \tag{2.16}$$

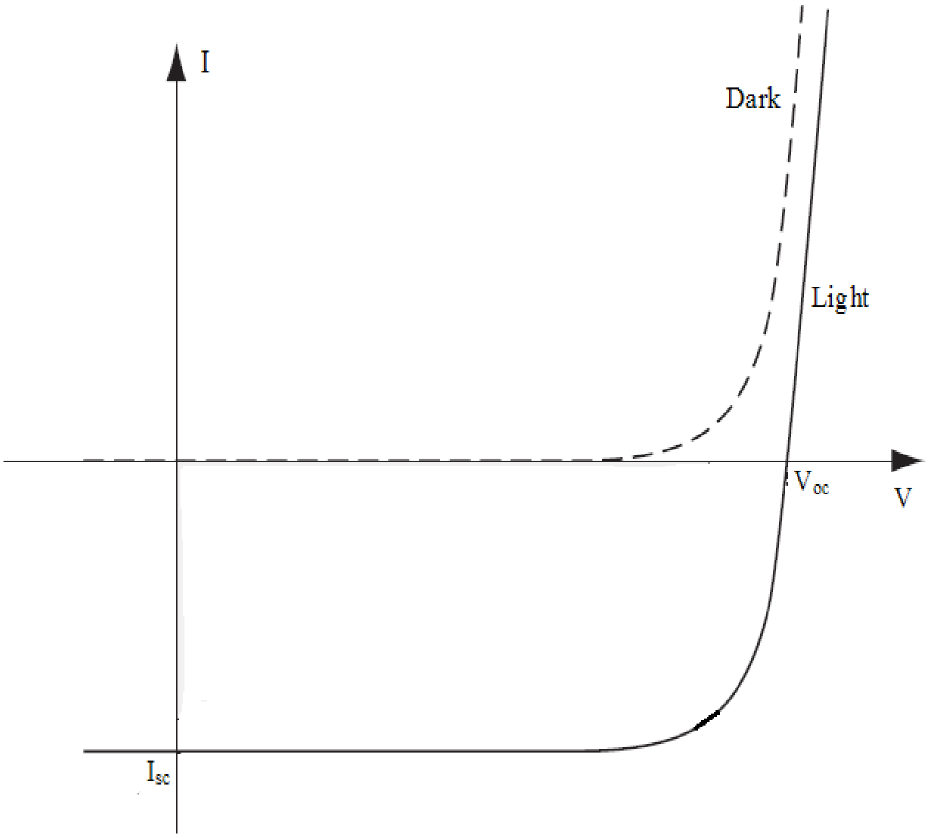

Figure 2.6 I-V characteristics under dark and illumined conditions [adapted from Möller, (1993)].

The reciprocal of the slope of the ln(I) vs. V curve gives the value of A, whereas the y intercept gives J_0. These two parameters are interrelated. The value of A usually lies between 1 and 2. The highest value of V_{oc} is obtained when I_0 is small. This normally corresponds to a value of 1 for A. The V_{oc} cannot be increased by increasing A as an increase in A leads to an increase in I_0, which affects V_{oc}. Figure 2.7 shows the maximum power or an inverted I-V curve of a solar cell in the fourth quadrant.

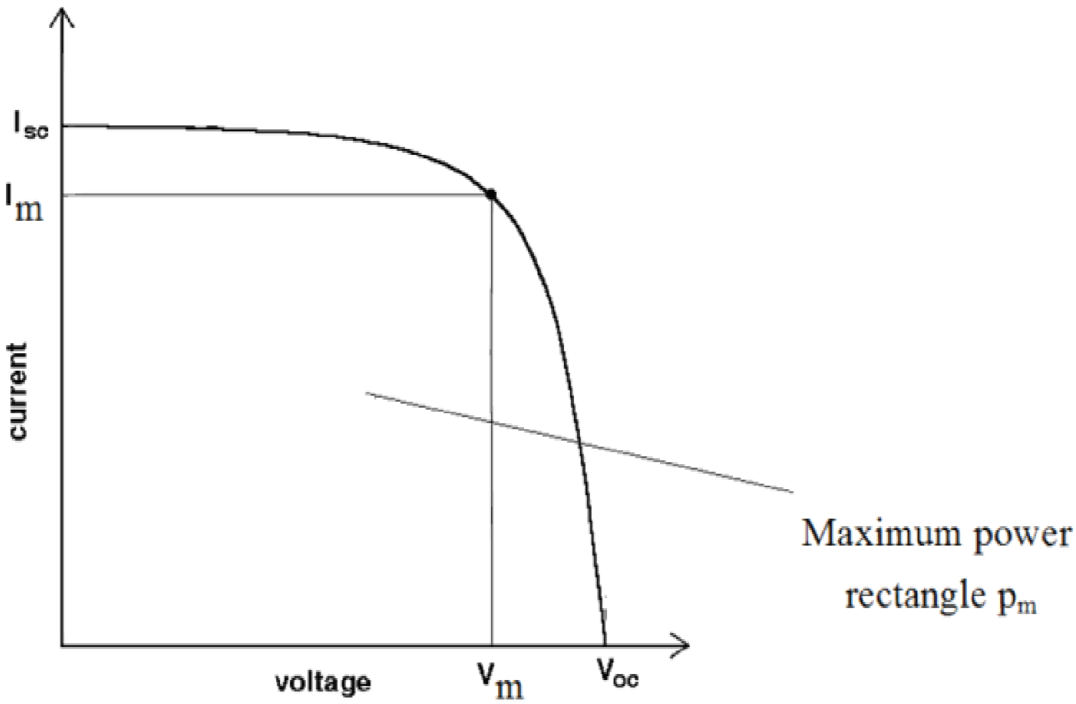

Figure 2.7 The inversion of an I-V curve showing the maximum power rectangle [adapted from Sze, (1981)].

The maximum power generated by a solar cell is equal to the maximum power point, which is the product of the voltage V_m and I_m. The fill factor (FF) of an I-V curve is defined by the following (Sze, 1981):

$$FF = \frac{V_m \, I_m}{V_{oc} \, I_{sc}} \tag{2.17}$$

The photovoltaic conversion efficiency is defined as a measure of the amount of light energy that is converted into electrical energy and is given by

$$\eta = \frac{P_m}{P_{in}} = \frac{FF \, I_{sc} \, V_{oc}}{P_{in}} \tag{2.18}$$

where P_m is the area of maximum power rectangle and P_{in} is the incident power.